Dentomaxillofacial Radiology (2015) 44, 20150078

birpublications.org/dmfr

RESEARCH ARTICLE

Effect of exposure parameters and voxel size on bone structure analysis in CBCT

[1,2]R Pauwels, [1]T Faruangsaeng, [1]T Charoenkarn, [1]N Ngonphloy and [1]S Panmekiate

[1]*Department of Radiology, Faculty of Dentistry, Chulalongkorn University, Bangkok, Thailand;* [2]*OMFS-IMPATH Research Group, Oral Imaging Center, Department of Imaging and Pathology, Biomedical Sciences Group, University of Leuven, Leuven, Belgium*

Objective: To evaluate the effect of exposure parameters and voxel size on bone structure analysis in dental CBCT.
Methods: 20 cylindrical bone samples underwent CBCT scanning (3D Accuitomo 170; J. Morita, Kyoto, Japan) using three combinations of tube voltage (kV) and tube current-exposure time product (mAs), corresponding with a CT dose index of 3.4 mGy: 90 kV and 62 mAs, 73 kV and 108.5 mAs, and 64 kV and 155 mAs. Images were reconstructed with a voxel size of 0.080 mm. In addition, the 90 kV scan was reconstructed at voxel sizes of 0.125, 0.160, 0.200, 0.250 and 0.300 mm. The following parameters were measured: bone surface (BS) and bone volume (BV) per total volume (TV), fractal dimension, connectivity density, anisotropy, trabecular thickness (Tb. Th.) and trabecular spacing (Tb. Sp.), structure model index (SMI), plateness, branches, junctions, branch length and triple points.
Results: For most parameters, there was no significant effect of the kV value. For BV/TV, "90 kV" differed significantly from the other kV settings; for SMI, "64 *vs* 73 kV" was significant. For BS/TV, fractal dimension, connectivity density, branches, junctions and triple points values incrementally decreased at larger voxel sizes, whereas an increase was seen for Tb. Th., Tb. Sp., SMI and branch length. For anisotropy and plateness, no (or little) effect of voxel size was seen; for BV/TV, the effect was inconsistent.
Conclusions: Most bone structure parameters are not affected by the kV if the radiation dose is constant. Parameters dealing with the trabecular structure are heavily affected by the voxel size.
Dentomaxillofacial Radiology (2015) **44**, 20150078. doi: 10.1259/dmfr.20150078

Cite this article as: Pauwels R, Faruangsaeng T, Charoenkarn T, Ngonphloy N, Panmekiate S. Effect of exposure parameters and voxel size on bone structure analysis in CBCT. *Dentomaxillofac Radiol* 2015; **44**: 20150078.

Keywords: cone beam CT; bone quality; trabecular bone; computer-assisted image processing

Introduction

CBCT has been widely used in dentistry to evaluate bone quality prior to implant placement and to diagnose and follow up various types of bony lesions.[1] Currently, bone evaluation is mainly limited to dimensional measurements[2] and a visual analysis of bone quality.[3] Owing to various issues related to the use of grey values in CBCT for absolute or relative density estimations,[4] alternative methods for quantitative bone analysis have been explored.[5]

Recently, the application of bone structure (or micro-architecture) analysis,[6] which has been used *ex vivo* on bone samples visualized in two dimension (histomorphometry) or three dimension (micro-CT),[7,8] has been considered for CBCT. Various studies have evaluated the correlation between bone parameters obtained through high-resolution micro-CT or CBCT scanning.[9–13] It was shown that, for certain parameters, a reasonable correlation can be seen, hinting towards a potential

Correspondence to: Dr Soontra Panmekiate. E-mail: Soontra.P@chula.ac.th
Financial support was received from the Faculty of Dentistry, Chulalongkorn University, Bangkok, Thailand.
Received 6 March 2015; revised 21 May 2015; accepted 8 June 2015

application in clinical practice. However, clinical application of bone structure analysis would only be feasible if the values of these parameters are independent from the scanning parameters used [*e.g.* tube voltage (kV), tube current-exposure time product (mAs) and voxel size]. If parameters have demonstrated stability under varying exposure conditions, it would be possible to determine classification schemes that can be used to distinguish healthy from pathological bone. Prior investigations have shown varying degrees of variability for a subset of bone structure parameters as a result of varying scan settings.[10,14,15] However, to our knowledge, an analysis of all available bone structure parameters on a larger ($n > 8$) sample has not yet been performed. Furthermore, the effect of tube voltage, which varies between 60 and 120 kV for CBCT scanners, on bone structure analysis has not yet been evaluated. Finally, more evidence is needed regarding the potential effect of voxel size (1) using a variety of voxel sizes ranging between small (<0.10 mm) and large (>0.25 mm) and (2) without varying other exposure parameters [*e.g.* field of view (FOV)].

The aim of this study was to evaluate the effect of exposure parameters and voxel size on bone structure analysis in dental CBCT.

Methods and materials

This study is a follow-up to previously published research,[9] in which the correlation between CBCT and micro-CT was evaluated. It involves the same bone samples and largely follows the same approach for image analysis.

The study protocol was approved by the Human Research Ethics Committee of the Faculty of Dentistry, Chulalongkorn University, Bangkok, Thailand (study code HREC-DCU 2015-012).

Sample preparation

20 dry hemimandibles with edentulous ridges posterior to the mental foramen were selected. A bone biopsy trephine bur was used for the removal of cylindrical samples of 2.8–2.9 mm diameter and variable length (10.7 ± 1.1 mm). Various samples were extracted from each hemimandible, after which one sample per hemimandible was retained through visual evaluation. The 20 bone samples were placed in styrofoam holders for CBCT scanning with their long axis perpendicular to the axial plane, corresponding to the orientation of an implant site.

CBCT scanning

Samples were scanned using the 3D Accuitomo 170 CBCT (J. Morita, Kyoto, Japan) using a FOV of 4 × 4 cm. Three combinations of kV and mAs, each with an exposure time of 30.8 s (*i.e.* 970 projections), were selected: 90 kV and 61.6 mAs, 73 kV and 107.8 mAs, and 64 kV and 154 mAs. The first exposure setting was determined in the previously mentioned study involving the same samples.[9] The others were selected in order to have a quasi-identical radiation dose, *i.e.* a CT dose index ($CTDI_{VOL}$) of 3.4 mGy.

Each scan was reconstructed at an isotropic voxel size of 0.080 mm. In addition, the projection data of the 90 kV scan was reconstructed at voxel sizes of 0.125, 0.160, 0.200, 0.250 and 0.300 mm (eliminating the effect of minor variation in tube and detector output, which would occur if new scans would be acquired for each voxel size).

Reconstructed images were exported as multifile digital imaging and communications in medicine data using a slice thickness and slice interval equal to the voxel size and converted into single-file tag image files for analysis using ImageJ (US National Institutes of Health, Bethesda, MD).

Cropping of CBCT images

Seeing that most of the FOV consisted of air, CBCT scans were cropped to cover the bone sample along with a minimal amount of air space. In the axial plane, each image was cropped to 3.6 × 3.6 mm (*i.e.* 45 x 45 voxels for the 0.080-mm scans). In the coronal/sagittal planes, the images were cropped according to the length of the sample. For each sample, the 0.080-mm scans were cropped identically. For the scans at other voxel sizes, cropping was performed to the nearest voxel (*e.g.* 29 × 29 voxels in the axial plane for the 0.125-mm scans, 23 × 23 voxels for the 0.160-mm scans etc.).

Thresholding

Following the study by Panmekiate et al,[9] all scans were thresholded and converted into a binary image using the stack-based "Moments" method developed by Tsai.[16] This is a fully automatic thresholding method (*i.e.* requiring no subjective user manipulation), in which the image moment is preserved. The *ith* moment m_i of an image can be expressed as:

$$m_i = \sum_j \frac{n_j}{n} (z_j)^i \quad (1)$$

where n_j is the number of pixels with a grey value of z_j, and n is the total number of pixels in the image. By matching the first three moments of the pre- and post-thresholded images, the algorithm ensures that high-density structures (*i.e.* high grey values, with a large contribution to the image moment) are distinguished from low-density structures (*i.e.* with a small contribution to the image moment).

Analysis of bone structure

The following bone structure parameters were measured using BoneJ, an ImageJ plugin (http://www.bonej.org):[17]

- Bone surface (BS) per total volume (TV) (BS/TV)[18]
- Bone volume per TV (BV/TV)
- Fractal dimension[19]
- Connectivity density (Conn. Dens.)[20,21]

- Anisotropy.[22,23] Because the calculation of this parameter involves a random component, the average value of 10 repeated calculations was used.
- Trabecular thickness (Tb. Th.) and trabecular spacing (Tb. Sp.)[24,25]
- Structure model index (SMI)[26]
- Plateness, an alternative for SMI, expressed as the ratio of eigenvalues (eV) along the longest (eV1), middle (eV2) and shortest (eV3) axis of the bone.
- Skeleton analysis.[27] The following parameters were included: branches, junctions, branch length and triple points.

Statistical analysis

Statistical analysis was performed using Prism 5.01 (GraphPad Software, San Diego, CA). For each bone parameter, normality of the distribution for the data points was evaluated using the D'Agostino–Pearson omnibus normality test. Paired *t*-tests, or Wilcoxon matched-pairs tests in case of non-normally distributed data, were performed to compare the scan settings two by two. Using a Bonferroni correction (considering the fact that 28 pairwise comparisons could be made between the eight scanning protocols), a significance level α of $0.05/28 = 0.0018$ was set.

Results

Figure 1 shows an axial slice of one of the samples for all eight scanning protocols, before and after thresholding. For the three 0.080-mm protocols with varying kV, little or no perceivable difference can be seen on the

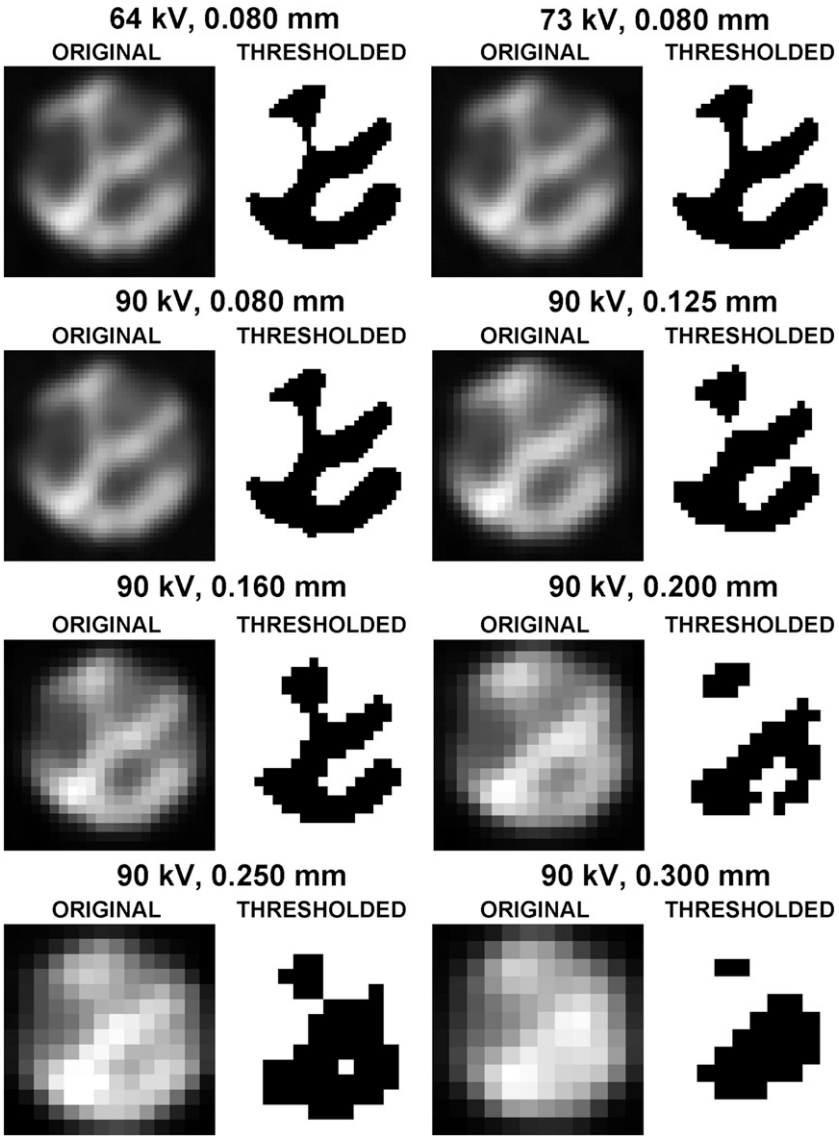

Figure 1 Eight CBCT scanning protocols. Axial slice of original and thresholded scans. Images were considerably enlarged.

original image, although the thresholded image shows a thinner trabecular branch for the 64-kV image. At larger voxel sizes, even as small as 0.125 mm, the images become increasingly blurry, and the trabecular structure gradually gets lost.

BS/TV, BV/TV and SMI passed the D'Agostino–Pearson omnibus normality test ($p > 0.05$) and were thus analysed using a paired *t*-test. All other parameters were analysed using the Wilcoxon matched-pairs test.

The distribution of the data for each scanning protocol is displayed using boxplots; in these plots and in the text below, the three 0.080-mm protocols are named according to their kV values (64, 73 and 90 kV), and the five other protocols are named according to the voxel size (0.125–0.300 mm). It should be emphasized that boxplots only display the distribution of the data; the fact that the data were paired was taken into account during statistical analysis.

Bone surface per total volume

Figure 2 shows the distribution of BS/TV values for each scanning protocol. The three kV settings show a similar distribution, but at larger voxel sizes, an incremental decrease in BS/TV can be seen. Pairwise comparisons revealed no significant differences for the three kV settings but showed significant differences for all pairs of protocols involving different voxel sizes.

Bone volume per total volume

Figure 2 shows the distribution of BV/TV values for each scanning protocol. Despite showing similar distributions, the "90-kV" protocol was significantly different from the lower kV settings. Overall, out of 28 pairwise comparisons between scanning protocols, 11 were significantly different. No consistent effect of voxel size on BV/TV values could be seen.

Fractal dimension

Figure 3 shows the distribution of fractal dimension values for each scanning protocol. No significant differences were seen between the three kV protocols as well as the "0.125-mm" protocol. At voxel sizes of 0.160 mm or above, increasingly lower fractal dimension values can be noticed, as well as wider distributions. All scan protocols with a voxel size of 0.160 mm or higher showed a significant difference with protocols involving voxel sizes of 0.125 mm or lower.

Connectivity density

Figure 4 shows the distribution of Conn. Dens. values for each scanning protocol. No significant differences were seen between the three kV protocols. Conn. Dens. consistently decreased at larger voxel sizes, showing significant differences for all pairwise comparisons involving a voxel size of 0.125 mm or higher, with the exception of the comparisons "64 kV *vs* 0.125 mm", "0.160 *vs* 0.200 mm" and "0.250 *vs* 0.300 mm".

Anisotropy

Figure 4 shows the distribution of anisotropy values for each scanning protocol. At voxel sizes of 0.125 mm or lower, more narrow distributions can be seen. No significant difference was found for any pairwise comparison of scanning protocols ($p > 0.0018$), although it can be noted that relatively low *p*-values (<0.05) were found for 9 out of 28 comparisons.

Trabecular thickness and trabecular spacing

Figure 4 shows the distribution of Tb. Th. and Tb. Sp. values for each scanning protocol. Tb. Th. values for different kV settings were stable ($p = 0.08$–0.52), while an incremental increase in thickness was seen at larger voxel sizes. Any pairwise comparison involving protocols with different voxel sizes revealed a significant difference.

Tb. Sp. showed a similar but less pronounced effect of voxel size. As with Tb. Th., the kV showed no significant effect on Tb. Sp. values. All comparisons involving different voxel sizes were significant, except those between the "0.160-mm", "0.200-mm" and "0.250-mm" protocols.

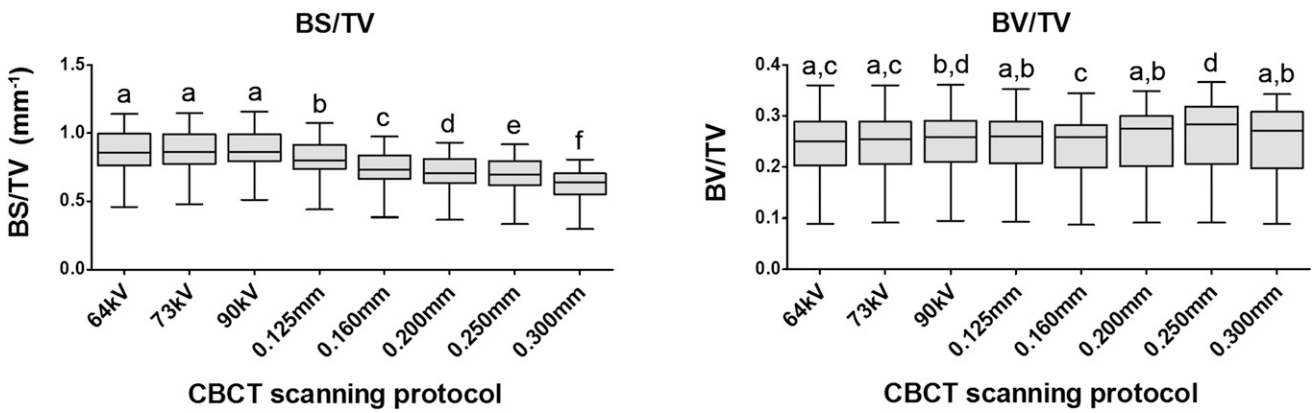

Figure 2 Distribution of BS/TV and BV/TV values for eight CBCT scanning protocols. Boxplots with different letters above them imply a significant difference (paired *t*-test, $p < 0.0018$). BS, bone surface; BV, bone volume; TV, total volume.

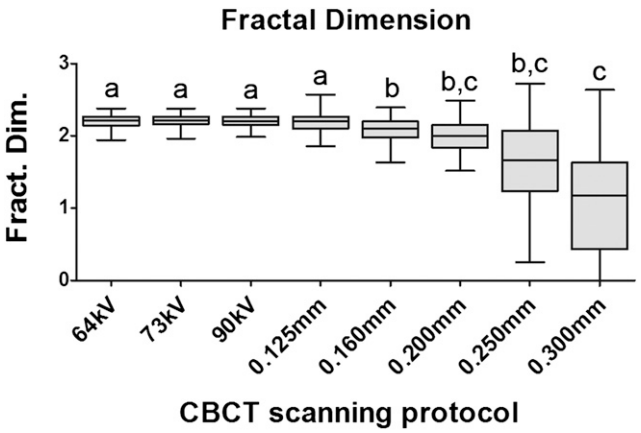

Figure 3 Distribution of fractal dimension (Fract. Dim.) values for eight CBCT scanning protocols. Boxplots with different letters above them imply a significant difference (Wilcoxon matched pairs, $p < 0.0018$).

Structure model index

Figure 5 shows the distribution of SMI values for each scanning protocol. The three kV protocols showed similar distributions, while larger voxel sizes resulted in increasingly higher SMI values (*i.e.* increased rod-like or decreased plate-like geometry) and more narrow distributions. For the three kV settings and the 0.125-mm setting, no significant differences were seen except for "64 *vs* 73 kV". All pairwise comparisons involving a voxel size of 0.160 mm or higher were significant except for "0.200 *vs* 0.250 mm". It can be noted that all 28 *p*-values for SMI were relatively low (<0.05).

Plateness

Figure 6 shows the distribution of eV2/eV1 and eV3/eV1 values for each scanning protocol. For eV2/eV1, no significant difference was seen among the eight scanning protocols ($p = 0.10$–0.91). For eV3/eV1, no differences were seen except for 0.250 mm, which showed a significant difference with all protocols except "0.200 mm" and "0.300 mm". A total of 16 out of 28 pairwise comparisons showed a *p*-value >0.0018 (*i.e.* the significance level with Bonferroni correction used in this study) but <0.05.

Skeleton analysis

Figure 7 shows the distribution of branches, junctions, branch length and triple points' values for each scanning protocol. Branches, junctions and triple points showed almost identical distributions. For these three

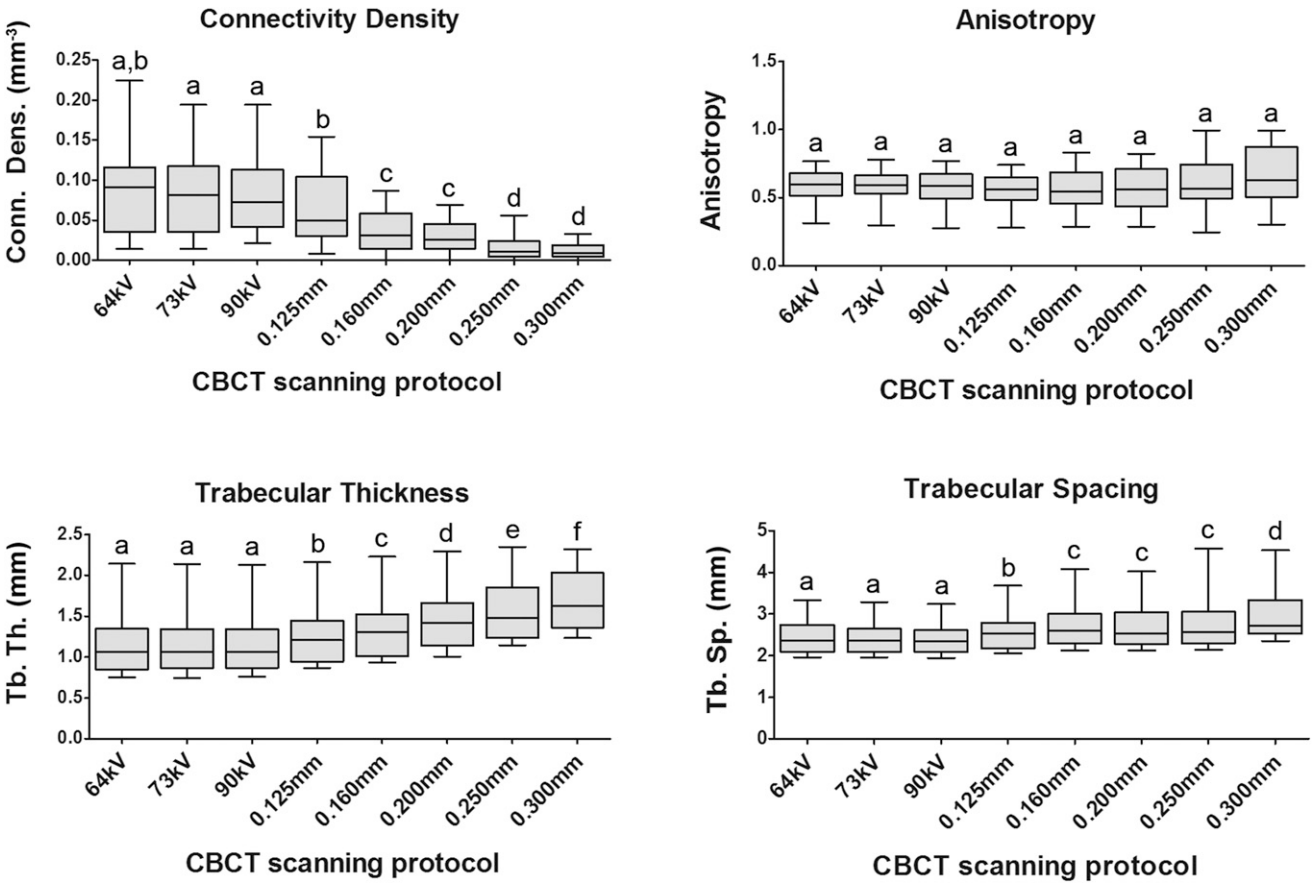

Figure 4 Distribution of connectivity density (Conn. Dens.), anisotropy, trabecular thickness (Tb. Th.) and trabecular spacing (Tb. Sp.) values for eight CBCT scanning protocols. Boxplots with different letters above them imply a significant difference (Wilcoxon matched pairs, $p < 0.0018$).

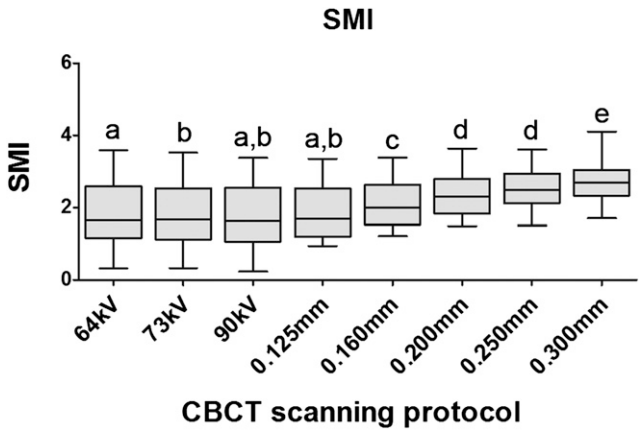

Figure 5 Distribution of structure model index (SMI) values for eight CBCT scanning protocols. Boxplots with different letters above them imply a significant difference (paired *t*-test, $p < 0.0018$).

parameters, no significant difference was found between the three kV protocols. However, all pairwise comparisons involving a voxel size of ≥0.125 mm were significant, showing increasingly lower branches/junctions/triple points' values at larger voxel sizes, with the exception of "0.250 *vs* 0.300 mm". Branch length distributions showed an opposite effect, with increasingly higher values at larger voxel sizes. No significant difference was found between the three kV settings, and all but three comparisons containing a voxel size ≥0.125 mm were significant.

Discussion

In this study, the effect of exposure parameters and voxel size on bone structure analysis in dental CBCT was evaluated. Various degrees of effects were seen for 14 bone structure parameters.

Small-sized samples, corresponding to the size of a typical region of interest for implant planning, were used in this study. Evidently, these samples do not represent a true clinical situation in terms of total scanned volume. Similarly, other studies have used mandibles (or sections thereof), with no simulation of the other hard and soft tissues of the head and neck[10–12,14,15] or rat femurs.[13] This leads to a reduced amount of X-ray absorption and scatter, which (in CBCT imaging) will mainly reflect itself as a lower image noise. In this study, this was compensated to a certain extent by reducing the tube output by 60% compared with that of an adult patient. Furthermore, it has been shown that moderate variations in noise (through the variation of tube output or the addition of water as a soft-tissue simulator) do not significantly affect bone structure parameters in CBCT.[10,15] Although it is possible that clinical scans will be somewhat more blurry owing to slight, yet, inevitable patient motion, *in vitro* experiments should be considered as a "best case scenario", reflecting the upper limit of what CBCT can currently achieve in terms of image quality. As elaborated upon further below, further study in a simulated or actual clinical setting is warranted before considering clinical application of bone structure parameters.

For most bone structure parameters included in this study, there was no significant effect of the kV value. The only exceptions were BV/TV, for which the 90-kV protocol differed significantly from the other two kV settings, and SMI, for which 64 *vs* 73 kV was significant. It should be noted that, for the three kV settings, the mA was adjusted accordingly in order to keep the radiation dose approximately constant. However, the kV affects the relative amount of scattered radiation and may thus lead to differences in noise. A phantom study by Pauwels et al,[28] using the same CBCT model as the present study, measured a higher contrast-to-noise ratio at higher kVs at a constant dose. While a higher noise may not significantly affect the segmentation of bone, the effect of kV may be more pronounced when larger samples are scanned than those used in this study. Van Dessel et al[10] compared bone structure parameters at 90 and 70 kV but, unlike the present study, did not fix the

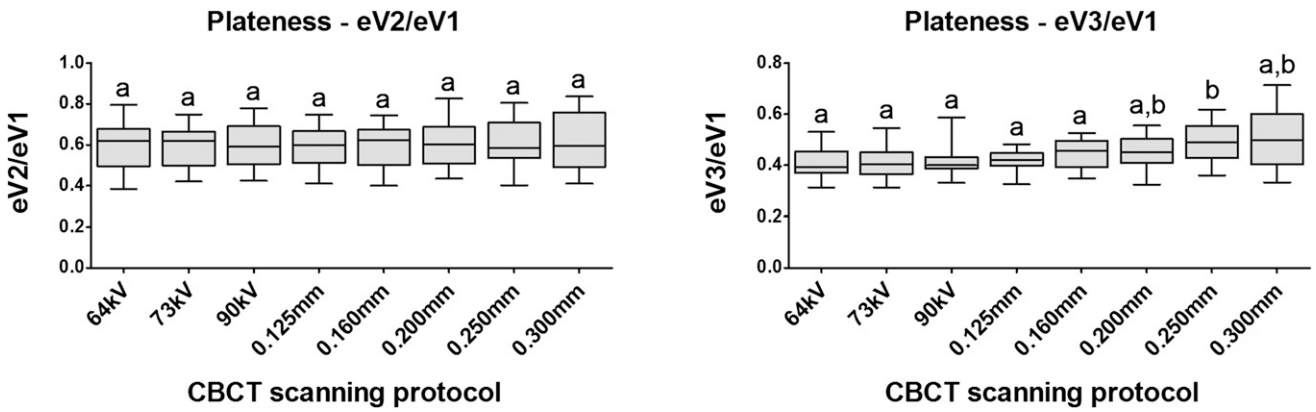

Figure 6 Distribution of eV2/eV1 and eV3/eV1 values for eight CBCT scanning protocols. Boxplots with different letters above them imply a significant difference (Wilcoxon matched pairs, $p < 0.0018$). eV, eigenvalues.

radiation dose (CT dose index: 3.4–8.1 mGy). They concluded that the effect of kV was not as pronounced as that of mA, as a lower correlation with micro-CT values was found for a high-kV, low-mA CBCT protocol.

Unlike kV, voxel size showed a significant effect on most bone parameters. This is in line with the decreased spatial resolution at larger voxel sizes,[29,30] leading to a loss of detail in the trabecular bone, which can be seen as a "merging" of neighbouring trabeculae. For anisotropy and plateness, no (or little) effect of voxel size was seen. These parameters do not require proper visualization of individual trabeculae, as long as the general structure is retained in the image. For BV/TV, no consistent effect was seen but several significant pairwise comparisons were found. It can be inferred that the effect of voxel size on BV/TV is somewhat unpredictable, as it may lead to an increase or decrease in volume depending on the actual bone structure. Dense bone with little or no pores would show little or no effect of voxel size, whereas porous bone could exhibit BV shifts in either direction. Figure 1 shows decreasing BV when voxel size increases up to 0.200 mm. The 0.250-mm scan shows an increased BV compared with the 0.200-mm scan, whereas BV for the 0.300-mm scan is decreased again.

As can be expected, for BS/TV, fractal dimension, Conn. Dens., branches, junctions and triple points, values incrementally decreased at larger voxel sizes, whereas an increase was seen for Tb. Th., Tb. Sp., SMI and branch length. In most cases, a significant effect was seen even for voxel sizes of 0.080 and 0.125 mm. While this may seem as only a small difference in voxel size, one must take into account that this number expresses the length of the edge of the cube-shaped voxels. When comparing the volume of the voxels instead, it can be calculated that a 0.080-mm voxel fits 3.8 times in a 0.125-mm voxel, 15.6 times in a 200-mm voxel and 52.7 times in a 300-mm voxel. While noise steadily increases at smaller voxel sizes if mAs is not increased accordingly,[30] it appears that the noise has a smaller effect on bone structure analysis than voxel size. Ibrahim et al showed no significant effect of CBCT exposure time, but a significant effect of voxel size (which was varied by changing the FOV size), on Tb. Th., Tb. Sp. and trabecular number (Tb. N.).[14,15] Van Dessel et al[10] showed that a 60% decrease in mA has little effect on bone structure parameters.

In recent years, increasing evidence has been published regarding the unreliability of grey values of CBCT.[31,32] The quantitative use of grey values for the

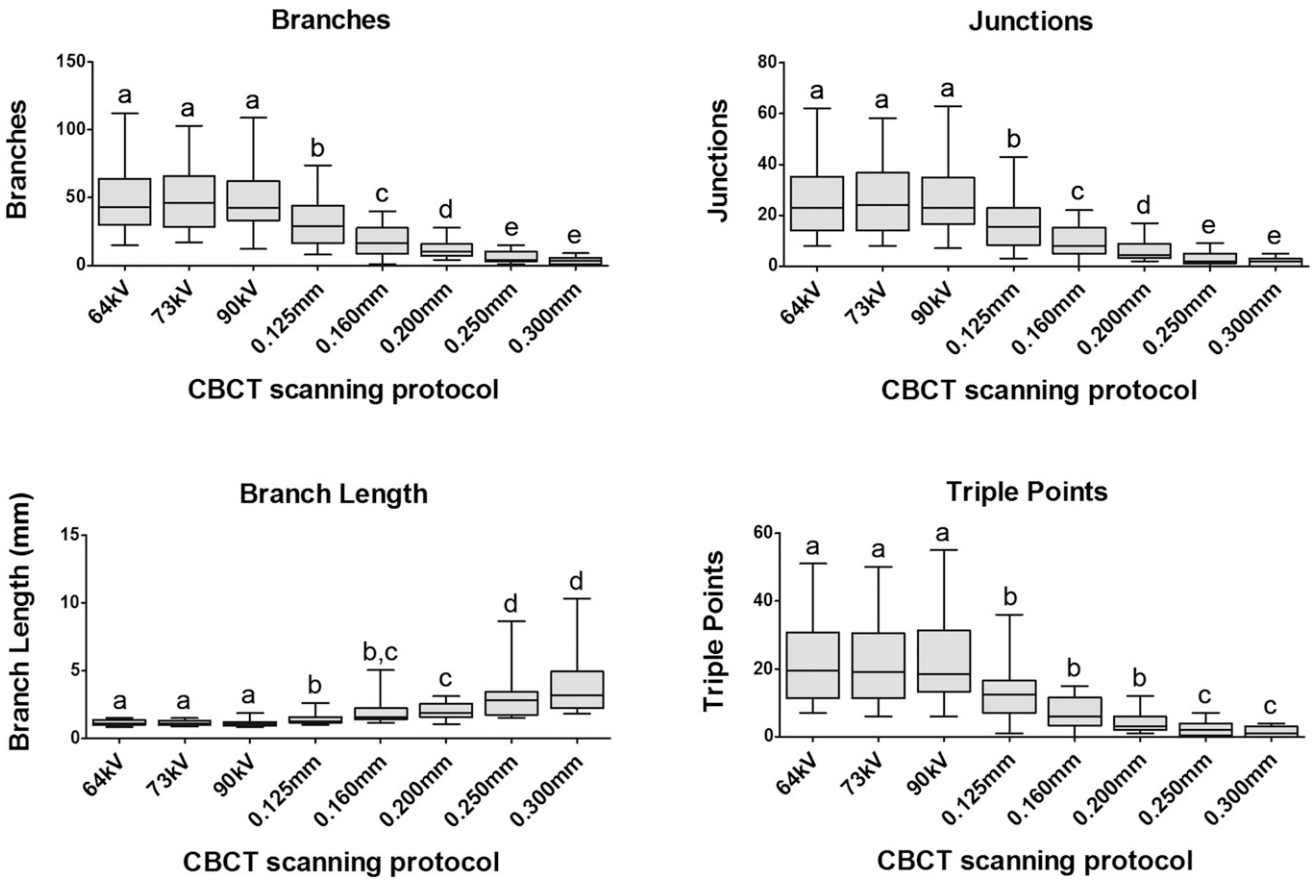

Figure 7 Distribution of branches, junctions, branch length and triple points' values for eight CBCT scanning protocols. Boxplots with different letters above them imply a significant difference (Wilcoxon matched pairs, $p < 0.0018$).

estimation of density, similar to the use of Hounsfield units in multidetector CT, should be generally avoided owing to the large variability between CBCT scans or between different regions of an individual scan.[4] In addition, the evaluation of bone quality has evolved from a density-based approach to a structural approach.[6] Hence, the potential application of bone structure parameters has gained attention. However, when combining the information from the present study with prior investigations, it can be concluded that some of these parameters may not be reliable, whereas others should be used with proper caution, as their values may be prone to a high unreliability. Considering clinical application, pilot studies have shown generally promising results regarding the use of fractal dimension in CBCT.[33,34] In an animal study, Huang et al[35] showed an effect of immediate *vs* delayed implant placement and loading on BS, Conn. Dens., Tb. Sp. and fractal dimension. Clinical investigation on the relation between bone structure parameters measured on CBCT images and clinical parameters (*e.g.* implant stability, success rate) is warranted. Such studies can be retrospective or prospective and should include patients for whom CBCT scanning is performed as part of a conventional treatment plan, seeing that the clinical evidence of the applicability of bone structure parameters is too limited to warrant exposing patients for experimental purposes. While these future studies should determine whether the clinical use of bone structure parameters is warranted, a few considerations can already be made. Widespread clinical application would require the determination of bone quality classification system(s) based on structural parameters, similar to existing visual or density-based classifications,[3,36] enabling the evaluation of bone quality and the selection of favourable implant sites (amongst others). At the moment, it seems doubtful that universal bone structure classifications can be determined owing to several reasons. First, values can differ considerably between CBCT models following the wide range in image quality.[29] Ibrahim et al[14] included two CBCT models in an evaluation of Tb. Th., Tb. Sp., Tb. N. and BV/TV of a human mandible. For all parameters, the two CBCTs showed different results, with one model showing overall lower values for Tb. Th. (−23%), Tb. Sp. (−15%), BV/TV (−16%) and higher values for Tb. N. (+23%). This implies that specific classification schemes may need to be established for each of the 50+ CBCT models currently being used in clinical practice. Second, most structural parameters are affected by the voxel size, as clearly demonstrated in this study. It remains to be seen whether a correction factor can be determined to take this into account. Third, results can vary depending on the analysis method used; particularly, the thresholding technique can have a large effect on the amount and the structure of "bone" in the binary image. In this study, 16 automatic thresholding techniques were visually evaluated before selecting the Moments method. Large variability was seen between these methods in terms of (1) the amount of bone thresholded, (2) the amount of fine structures retained in the thresholded image and (3) the amount of noise in the thresholded image. Ideally, this aspect of the analysis should be standardized at some point. Finally, classification schemes should be future-proof; it can be expected that the ever-increasing image quality of CBCT, owing to the use of new or optimized hardware and software, will lead to a more accurate representation of the true bone structure (similar to micro-CT). This may imply that classifications based on structural parameters would have to be periodically reviewed.

In conclusion, most bone structure parameters are not sensitive to the kV if the radiation dose is constant. Parameters dealing with the trabecular structure rather than the bone as a whole are affected by the voxel size, even at voxel sizes of $\leq$0.125 mm. Clinical validation of the use of CBCT for measuring bone structure parameters is warranted before widespread application can be considered.

References

1. Scarfe WC, Farman AG, Sukovic P. Clinical applications of cone-beam computed tomography in dental practice. *J Can Dent Assoc* 2006; **72**: 75–80.
2. Kosalagood P, Silkosessak OC, Pittayapat P, Pisarnturakit P, Pauwels R, Jacobs R. Linear measurement accuracy of eight cone beam computed tomography scanners. *Clin Implant Dent Relat Res* Mar 2014. Epub ahead of print. doi: 10.1111/cid.12221
3. Lindh C, Petersson A, Rohlin M. Assessment of the trabecular pattern before endosseous implant treatment: diagnostic outcome of periapical radiography in the mandible. *Oral Surg Oral Med Oral Pathol Oral Radiol Endod* 1996; **82**: 335–43. doi: 10.1016/S1079-2104(96)80363-5
4. Pauwels R, Jacobs R, Singer SR, Mupparapu M. CBCT-based bone quality assessment: are Hounsfield units applicable? *Dentomaxillofac Radiol* 2015; **44**: 20140238. doi: 10.1259/dmfr.20140238
5. Ribeiro-Rotta RF, de Oliveira RC, Dias DR, Lindh C, Leles CR. Bone tissue microarchitectural characteristics at dental implant sites part 2: correlation with bone classification and primary stability. *Clin Oral Implants Res* 2014; **25**: e47–53. doi: 10.1111/clr.12046
6. Wirth AJ, Goldhahn J, Flaig C, Arbenz P, Müller R, van Lenthe GH. Implant stability is affected by local bone microstructural quality. *Bone* 2011; **49**: 473–8. doi: 10.1016/j.bone.2011.05.001
7. González-García R, Monje F. Is micro-computed tomography reliable to determine the microstructure of the maxillary alveolar bone? *Clin Oral Implants Res* 2013; **24**: 730–7. doi: 10.1111/j.1600-0501.2012.02478.x
8. Müller R, Van Campenhout H, Van Damme B, Van Der Perre G, Dequeker J, Hildebrand T, et al. Morphometric analysis of human bone biopsies: a quantitative structural comparison of histological sections and micro-computed tomography. *Bone* 1998; **23**: 59–66. doi: 10.1016/S8756-3282(98)00068-4
9. Panmekiate S, Ngonphloy N, Charoenkarn T, Faruangsaeng T, Pauwels R. Comparison of mandibular bone microarchitecture between micro-CT and CBCT images. *Dentomaxillofac Radiol* 2015; **44**: 20140322. doi: 10.1259/dmfr.20140322
10. Van Dessel J, Huang Y, Depypere M, Rubira-Bullen I, Maes F, Jacobs R. A comparative evaluation of cone beam CT and micro-CT on trabecular bone structures in the human mandible. *Dentomaxillofac Radiol* 2013; **42**: 20130145. doi: 10.1259/dmfr.20130145

11. Parsa A, Ibrahim N, Hassan B, van der Stelt P, Wismeijer D. Bone quality evaluation at dental implant site using multislice CT, micro-CT, and cone beam CT. *Clin Oral Implants Res* 2015; **26**: e1–7. doi: 10.1111/clr.12315
12. Ibrahim N, Parsa A, Hassan B, van der Stelt P, Aartman IH, Wismeijer D. Accuracy of trabecular bone microstructural measurement at planned dental implant sites using cone-beam CT datasets. *Clin Oral Implants Res* 2014; **25**: 941–5. doi: 10.1111/clr.12163
13. Hsu JT, Wang SP, Huang HL, Chen YJ, Wu J, Tsai MT. The assessment of trabecular bone parameters and cortical bone strength: a comparison of micro-CT and dental cone-beam CT. *J Biomech* 2013; **46**: 2611–18. doi: 10.1016/j.jbiomech.2013.08.004
14. Ibrahim N, Parsa A, Hassan B, van der Stelt P, Aartman IH, Nambiar P. Influence of object location in different FOVs on trabecular bone microstructure measurements of human mandible: a cone beam CT study. *Dentomaxillofac Radiol* 2014; **43**: 20130329. doi: 10.1259/dmfr.20130329
15. Ibrahim N, Parsa A, Hassan B, van der Stelt P, Aartman IH, Wismeijer D. The effect of scan parameters on cone beam CT trabecular bone microstructural measurements of human mandible. *Dentomaxillofac Radiol* 2013; **42**: 20130206. doi: 10.1259/dmfr.20130206
16. Tsai WH. Moment-preserving thresholding: a new approach. *Comput Vis Graph* 1985; **29**: 377–93. doi: 10.1016/0734-189X(85)90133-1
17. Doube M, Kłosowski MM, Arganda-Carreras I, Cordelières FP, Dougherty RP, Jackson JS, et al. BoneJ: free and extensible bone image analysis in ImageJ. *Bone* 2010; **47**: 1076–9. doi: 10.1016/j.bone.2010.08.023
18. Lorensen WE, Cline HE. Marching cubes: a high resolution 3D surface construction algorithm. Proceedings of the 14th Annual Conference on Computer Graphics and Interactive Techniques; Anaheim, CA. New York, NY: ACM, 1987. pp. 163–9.
19. Fazzalari NL, Parkinson IH. Fractal dimension and architecture of trabecular bone. *J Pathol* 1996; **178**: 100–5. doi: 10.1002/(SICI)1096-9896(199601)178:1<100::AID-PATH429>3.0.CO;2-K
20. Odgaard A, Gundersen HJ. Quantification of connectivity in cancellous bone, with special emphasis on 3-D reconstructions. *Bone* 1993; **14**: 173–82. doi: 10.1016/8756-3282(93)90245-6
21. Toriwaki J, Yonekura T. Euler number and connectivity indexes of a three dimensional digital picture. *Forma* 2002; **17**: 183–209.
22. Odgaard A. Three-dimensional methods for quantification of cancellous bone architecture. *Bone* 1997; **20**: 315–28. doi: 10.1016/S8756-3282(97)00007-0
23. Harrigan TP, Mann RW. Characterization of microstructural anisotropy in orthotropic materials using a second rank tensor. *J Mater Sci* 1984; **19**: 761–7. doi: 10.1007/BF00540446
24. Dougherty R, Kunzelmann KH. Computing local thickness of 3D structures with ImageJ. *Microsc Microanal* 2007; **13**: 1678–9. doi: 10.1017/S1431927607074430
25. Hildebrand T, Rüegsegger P. A new method for the model-independent assessment of thickness in three-dimensional images. *J Microsc* 1997; **185**: 67–75. doi: 10.1046/j.1365-2818.1997.1340694.x
26. Hildebrand T, Rüegsegger P. Quantification of bone microarchitecture with the structure model index. *Comput Methods Biomech Biomed Engin* 1997; **1**: 15–23. doi: 10.1080/01495739708936692
27. Arganda-Carreras I, Fernández-González R, Muñoz-Barrutia A, Ortiz-De-Solorzano C. 3D reconstruction of histological sections: application to mammary gland tissue. *Microsc Res Tech* 2010; **73**: 1019–29. doi: 10.1002/jemt.20829
28. Pauwels R, Silkosessak O, Jacobs R, Bogaerts R, Bosmans H, Panmekiate S. A pragmatic approach to determine the optimal kVp in cone beam CT: balancing contrast-to-noise ratio and radiation dose. *Dentomaxillofac Radiol* 2014; **43**: 20140059. doi: 10.1259/dmfr.20140059
29. Pauwels R, Beinsberger J, Stamatakis H, Tsiklakis K, Walker A, Bosmans H, et al; SEDENTEXCT Project Consortium. Comparison of spatial and contrast resolution for cone-beam computed tomography scanners. *Oral Surg Oral Med Oral Pathol Oral Radiol* 2012; **114**: 127–35. doi: 10.1016/j.oooo.2012.01.020
30. Pauwels R, Araki K, Siewerdsen JH, Thongvigitmanee SS. Technical aspects of dental CBCT: state of the art. *Dentomaxillofac Radiol* 2015; **44**: 20140224. doi: 10.1259/dmfr.20140224
31. Pauwels R, Nackaerts O, Bellaiche N, Stamatakis H, Tsiklakis K, Walker A, et al; SEDENTEXCT Project Consortium. Variability of dental cone beam CT grey values for density estimations. *Br J Radiol* 2013; **86**: 20120135. doi: 10.1259/bjr.20120135
32. Molteni R. Prospects and challenges of rendering tissue density in Hounsfield units for cone beam computed tomography. *Oral Surg Oral Med Oral Pathol Oral Radiol* 2013; **116**: 105–19. doi: 10.1016/j.oooo.2013.04.013
33. González-Martín O, Lee EA, Veltri M. CBCT fractal dimension changes at the apex of immediate implants placed using undersized drilling. *Clin Oral Implants Res* 2012; **23**: 954–7. doi: 10.1111/j.1600-0501.2011.02246.x
34. Torres SR, Chen CS, Leroux BG, Lee PP, Hollender LG, Schubert MM. Fractal dimension evaluation of cone beam computed tomography in patients with bisphosphonate-associated osteonecrosis. *Dentomaxillofac Radiol* 2011; **40**: 501–5. doi: 10.1259/dmfr/14636637
35. Huang Y, Van Dessel J, Liang X, Depypere M, Zhong W, Ma G, et al. Effects of immediate and delayed loading on peri-implant trabecular structures: a cone beam CT evaluation. *Clin Implant Dent Relat Res* 2014; **16**: 873–83. doi: 10.1111/cid.12063
36. Misch CE. Density of bone: effect on treatment plans, surgical approach, healing, and progressive bone loading. *Int J Oral Implantol* 1990; **6**: 23–31.